JOURNAL OF MATERIALS SCIENCE 26 (1991) 1769–1774

Thermal characterization of amorphous selenium films obtained by low-temperature photodeposition

A. PELED
Center for Technological Education, aff. Tel-Aviv University, 52 Golomb St., Holon 58368, Israel

E. HADZIIOANNOU
Department of Polymer Chemistry, University of Groningen, Nijenborgh 16, 9747 AG, Groningen, The Netherlands

The thermal treatment structural behaviour of amorphous selenium (a–Se) films as obtained by a low-temperature photodeposition process was studied. Differential scanning calorimetry (DSC) measurements were used to obtain detailed information regarding the structural changes in the temperature range of − 50–250 °C. Our understanding of the crystallization behaviour was also aided by scanning electron microscopy (SEM) and X-ray diffraction analysis (XRD). The results were compared to other observations made on structural transitions of a–Se obtained traditionally by high-temperature processes such as quenching from the melt and vacuum deposition. Comparing the DSC thermograms clearly shows that the low-temperature photodeposition process gives a different structural transition behaviour of a–Se during thermal crystallization. Specifically new transitions were observed structurally in the temperature range 80–160 °C.

1. Introduction

Selenium in its solid state phase co-exists at room temperature in four different allotropic forms: α-monoclinic, β-monoclinic, h c p-hexagonal (trigonal) and amorphous [1–4]. The red amorphous selenium (a–Se) phase is obtained by chemical [5], electrochemical [6] or vacuum deposition processes [7–9]. It has also been reported that a–Se is unstable at temperatures above 30 °C where it undergoes a glass transition [3, 5] and even grey crystalline Se is partially formed [9]. Also a–Se crystallizes above room temperature to the hexagonal crystalline allotrope at various time rates. Several crystallization onset temperatures have been reported in the literature in the range 30–130 °C [10] but they were never properly defined, since, for every investigated case the phase transition or structural change was dependent on many factors, such as impurity agents and their relative concentration [10]. The thermal treatment period and the preparation procedure of the a–Se samples are also examples of the multitude of factors involved in the crystallization rate and its onset temperature. Besides being of theoretical interest, the topic of amorphous to crystalline transformation has recently received much attention due to several novel scientific and technological applications, mainly in the domain of nonmagnetic recording media. Many of the previous works on the crystallization kinetics of a–Se were motivated by the Xerographic industry which was interested mainly in a–Se layers which were highly resistant to crystallization. In recent years, however, such transitions have also found applications in the new emerging technology of optical recording [11].

2. The microstructure of the solid phase of Se

It has already been established [7] that selenium in the molten or liquid state structurally consists of a mixture of 30–50% Se_8 rings and Se_x chains of various lengths which are in thermal dynamic equilibrium. Quite generally, the ring number and average chain length decrease as the temperature is increased. This is the reason why various quenching processes of a–Se from the melt result in different ring and chain proportion in the solid phase [1]. Similarly, one might also expect significant differences in the relative proportion of Se_8 rings and Se_x chains for vacuum evaporated films as compared to chemically deposited a–Se films which are prepared at low temperatures. The photodeposition of a–Se [13] can be classified accordingly as a low temperature deposition process, since it involves precipitation and colloid aggregation in aqueous solutions. Structural investigations have shown [4] that selenium chains join to form the hexagonal (trigonal) crystalline phase. This process occurs predominantly at relatively high temperatures, above approximately 120 °C while rings form the monoclinic α and β crystalline phases at low temperatures such as room temperature or lower. It was also

0022–2461/91 $03.00 + .12

reported that the glassy or amorphous phase consists of various mixtures of these two microstructures, i.e. rings and chains. However, unlike the molten state, they are not supposed to be in thermal equilibrium but rather in a frozen metastable state created by the specific quenching [3] method of solidification used.

The chain microstructure consists of atoms arranged in helices which in the trigonal crystalline phase are oriented along the *c*-axis of the elementary cell [14], each forming covalent bonds with nearest neighbours so that each atom has an octet of valence electrons. The chains are held together by the relative weak Van-der-Waals forces and the cleavage planes are parallel to the chain axis. This structure is highly unisotropic, as would be expected from the two types of bonding, perpendicular and parallel to the *c*-axis. The helical chain is surrounded by six nearest neighbour helices located at the six corners of a hexagon, to yield a 3-dimensional structure. The intrachain is much stronger than the interchain bonding but the 3-dimensional hexagonal crystal is still believed to be stabilized predominantly by the weaker Van-der-Waals interchain forces. This conclusion was drawn, for instance, from the pressure influence [4, 14] which leads to a lower electrical resistivity, presumably due to closer packing of the crystalline structure. The structure of α-monoclinic crystals [15] is quite different. The basic unit is a Se_8 ring molecule, four such molecules forming a unit cell. The β-monoclinic is different from the α-phase only in a modified stacking pattern resulting in different interatomic distances [15]. Radial distribution analysis [7, 16] has suggested that conversion of the selenium from ring to chain symmetry occurs by ring opening. From such considerations, it can be concluded that rings are probably created either at very low temperatures or in the molten state. Otherwise, the rings are more prone to opening leading to the chain structural form.

2.1. Scanning electron microscopy : structural analysis of the photodeposited films

The photodeposited a–Se films were analysed structurally by SEM at various stages of the photodeposition process and described previously [17]. In Fig. 1, we show only the freshly-obtained film structure and those which are subsequently partially crystallized by thermal treatments. An amorphous structure is observed in Fig. 1a while individual hexagonal microcrystals can be seen in Fig. 1b. The crystallization in this case was initiated by heating the amorphous film to a temperature of 70 °C. It was observed that only grey hexagonal crystallization occurred.

2.2. X-ray diffraction analysis

This method was used to observe the crystallinity of thermally-treated specimens of a–Se films. Two typical XRD diffractograms are shown in Fig. 2. Fig. 2a related to an untreated film which is also shown in Fig. 1a. Fig. 2b relates to the same specimen after thermal treatment in which one may observe the appearance of well defined peaks which pertain to the crystalline hexagonal phase. Actually, since the peaks are rather broad, it indicates that the film is only partially crystallized as one can also see from Fig. 1b.

2.3. Differential scanning calorimetry

Red amorphous selenium material was photodeposited on glass substrates using the usual procedures described earlier [18]. A Du Pont 1090 Differential Scanning Calorimeter (DSC) was used for the dynamic heating experiments. All samples were scraped from the glass substrate and inserted in small, sealed aluminium pans. Typical charges used were about 10–20 mg. It was immediately observed that the DSC scans obtained from the as-photodeposited films were

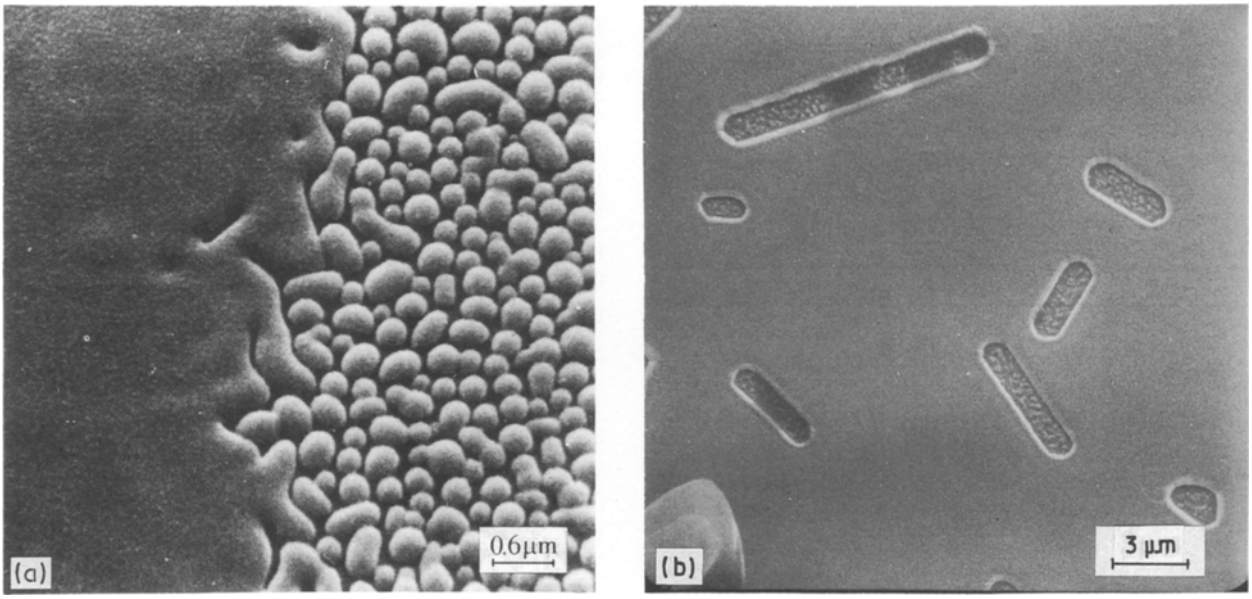

Figure 1 (a) SEM microstructure of a thin film sample of a–Se as-obtained by the photodeposition process at 10 °C. Half of the picture shows a discontinuous film which consists of partially merged spheroidal islands; (b) A SEM picture of partially crystallized amorphous film. Note the formation of needle shaped hexagonal crystallites within the amorphous phase.

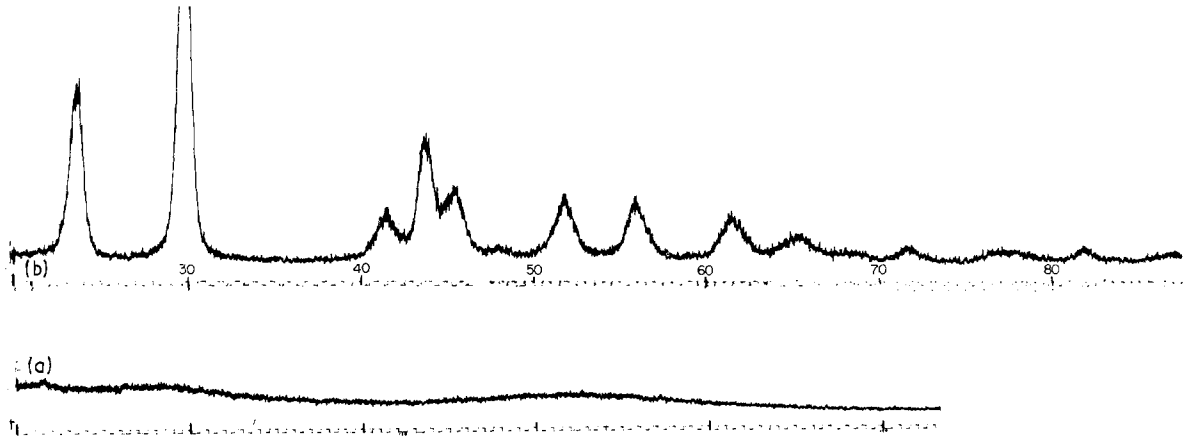

Figure 2 (a) XRD scan of an amorphous Se film obtained by photodeposition; (b) XRD scan for a partially crystallized a–Se film formed by heating an amorphous sample to 70 °C.

different and of a complex peak structure as compared to rescanned samples performed after cycling the temperature linearly from − 50 °C to 250 °C. Hence, it was decided to take subsequent thermographs by using several cooling rates while keeping the heating rate at a constant of 5 °C min^{-1}. In Figs 3, 4 and 5 we show a sequence of three thermographs with different thermal treatment history. The DSC trace in Fig. 3 was obtained for a virgin-photodeposited a–Se sample which was precipitated at 10 °C and kept at room temperature for several days. Several other virgin samples, run through the same range of temperatures, gave basically the same complex patterns as shown in Fig. 3. Quite generally we observe the occurrence of one endotherm peak at $T_{\mathrm{I}}^{\mathrm{EN}} \simeq 47$ °C. Then two exotherms follow at $T_{\mathrm{I}}^{\mathrm{EX}} \simeq 95$ °C and at $T_{\mathrm{II}}^{\mathrm{EX}} \simeq 154$ °C and finally a sharply defined endotherm peak at $T_{\mathrm{II}}^{\mathrm{EN}} \simeq 222$ °C. Two additional shoulders are also observed between 115–140 °C. Such a thermal behaviour of a–Se material is interesting since no such complex peaks have ever been reported [19, 20] or observed for a–Se material obtained by high temperature quenching or vaccum deposition methods. In fact, the DSC thermograms of vacuums a–Se films only exhibit one small endothermic peak at about 46 °C and a simple broad exothermic peak at about 120 °C [19]. However

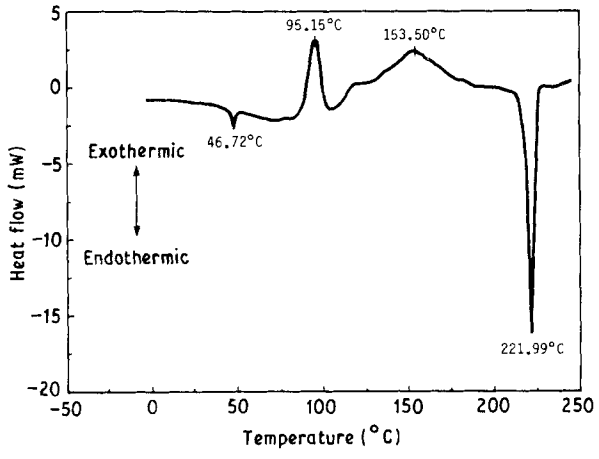

Figure 3 DSC thermogram for a photodeposited a–Se sample at 10 °C; weight: 15.8 mg; scan rate; 5 °C min^{-1}.

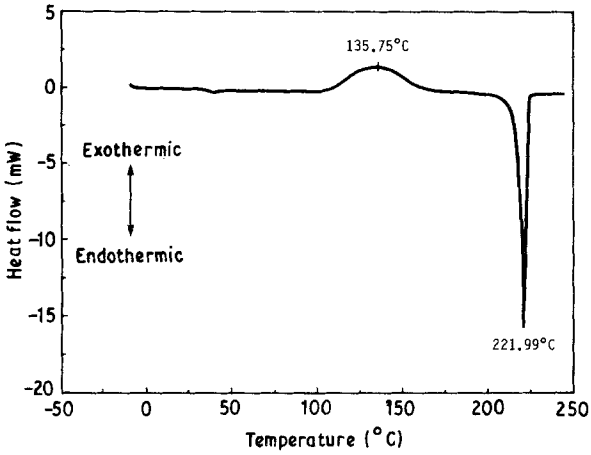

Figure 4 DSC thermogram of the sample in Fig. 3 after quenching from 250 to − 50 °C at a rate of 5 °C min^{-1}.

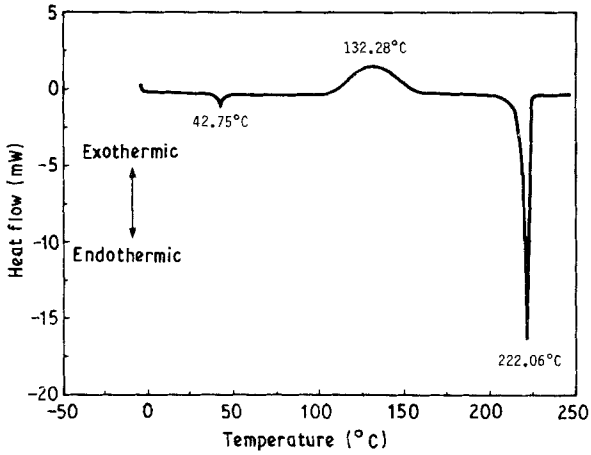

Figure 5 DSC thermogram of the sample in Fig. 4 after quenching from 250 to − 50 °C at a rate of 50 °C min^{-1}.

for thermally treated samples such as the DSC traces of Figs 3 and 4, are similar to those published in the literature [19, 20]. Since Fig. 4 includes one endothermic peak and one exothermic peak before the melt, it seems that this thermal quench creates a very similar structure to the vacuum deposited films. Also, the complex feature exhibited in the DSC thermograms of Fig. 3 could not be reproduced by any subsequent thermal treatments. This points out the very important result that low-temperature deposition processes create a very special microstructural combination of chains and rings which is destroyed as soon as one cycles the temperature up to the melt. Finally, we observe in Figs 3, 4 and 5 the sharp endothermic peak at about 220 °C, the melting point of selenium.

3. Discussion

The DSC thermograms given in Figs 3, 4 and 5 show the effect of thermal treatment on the structural properties of a–Se as obtained by the low-temperature photodeposition process. Quite general features are exhibited in Fig. 3 which shows complex a–Se transformation steps in the crystallization temperature region prior to its melting at 220 °C. In Table I we present all the important endothermic and exothermic transition parameters for the thermograms given in Figs 3, 4 and 5. Onset temperatures T_{onset} are determined in the usual manner from the intercept of the extrapolated base and a line drawn tangentially to the transition portion of the curve at maximum slope. The peak temperatures T_{peak} are obtained for the same transitions wherever there is a well defined peaked curve. Finally, the heats of transitions, ΔH, in (J g^{-1}) are obtained from the integral of the curves for every transition peak taken from the baseline.

It is simpler to analyse the endotherm at $T = 222$ °C first, since we can clearly relate it to the melting process which has been observed in many works at about $T_m \simeq 220$ °C. The transition heat from Table I gives about 0.047 (eV atom^{-1}) or 1.09 (kcal mol^{-1}). At this temperature those values mean that every Se atom requires on average about $\simeq kT$ energy to transform to the liquid form. It is also easy to recognize the endothermic transition peak at $T = 47$ °C since it is very close to the glass transition peak given in several papers [3, 5, 19–21] in the range $T_g \simeq 30$–47 °C. Actually, it has been shown that T_g depends on the thermal treatment or material preparation procedures and one may also attribute some of the differences to the definition of the glass transition temperature on the DSC curve. The calculation for the average transition energy gives about 0.002 (eV atom^{-1}) or 0.044 (kcal mol^{-1}) for this endothermic transition. This value is about (1/14)kT per atom for the softening process of the glassy Se through T_g. Such a small heat content means that an average chain length of about 14 atoms is able to absorb enough thermal energy to allow the new structural adjustment needed to acquire the new degree of freedom, above T_g. It may also be possible that at this temperature only the ring members of the a–Se mixture acquire this new degree of freedom and not the long chains which contain about

TABLE I Peak temperatures T_{peak}, onset temperature T_{onset}, and transition heats ΔH, for the structural transition DSC curves. Data obtained with a computerized system General V4.OD connected to a DSC instrument (*DuPont* 2100). T_g, T_c and T_m denote glass transition, crystallization and melting temperatures, respectively.

Sample	Endotherm-I			Exotherm-I			Exotherm-II			Endotherm-II		
	T_{peak} (°C)	T_{onset} (°C)	ΔH (j g^{-1})	T_{peak} (°C)	T_{onset} (°C)	ΔH (j g^{-1})	T_{peak} (°C)	T_{onset} (°C)	ΔH (j g^{-1})	T_{peak} (°C)	T_{onset} (°C)	ΔH (j g^{-1})
As-photodeposited	46.72	44.34	2.327	95.15	87.53	30.39	153.50	133.48	51.48	222	218.12	58.00
I-quench	40.00	38.00	0.200	–	–	–	135.75	110.00	43.92	222	218.18	52.00
II-quench	42.75	39.67	2.038	–	–	–	132.28	108.73	42.43	222	218.21	52.49
	$T_g \simeq 38.44$ °C			$T_{c_1} \simeq 88$ °C			$T_{c_2} \simeq 132$–153 °C			$T_m \simeq 220$ °C		

10^5 atoms each [12]. Such a long chain is obviously too large to allow significant chain movement at such a low temperature. This hypothesis is strengthened further by the observation that in Fig. 4 the glass transition is almost negligible, as if no softening of the glassy matrix occurs through $T \simeq 46\,^{\circ}C$. For this specific structural transition, the low quenching rate of $5\,^{\circ}C\,min^{-1}$ gives an average transition energy of only about $(1/200)kT$ per atom which may mean that the ring population is scarce as compared to the virgin sample. However, for the fast quenching experiments such as the one given in Fig. 5 we again obtain heat transitions of about $(1/16)kT$ per atom at T_g, very close to the value obtained for the virgin-photodeposited samples. Hence, we observe that reversibility of the T_g transition can be achieved only for fast quenching rates of $50\,^{\circ}C\,min^{-1}$ or more. Such a T_g transformation behaviour may obviously be of interest in bistable memory devices such as optical storage devices in which lasers may write/erase several times a pixel in a Se film array by thermally creating or destroying the endothermic peak at T_g, see Figs 4 and 5.

The next two exotherms in Fig. 3, at $T_I^{EX} \simeq 95\,^{\circ}C$ and $T_{II}^{EX} \simeq 154\,^{\circ}C$ are probably related to the crystallization process of a–Se. The high-temperature transition peak at $T_{II}^{EX} \simeq 154\,^{\circ}C$ is surely the crystalline transition process to the hexagonal phase since any sample beyond this point is converted to the easily-recognized grey crystalline film. The surprising result, however, is the transition which occurs at $T_I^{EX} \simeq 95\,^{\circ}C$ and the shoulders between those two peaks.

First, we observe that such a complex thermogram has never been obtained before [19, 20] and even our quenched samples do not exhibit this pattern after the first temperature cycling up to the melting point, see Figs 4 and 5. The average value of T_I^{EX} and T_{II}^{EX} actually give a value of about $124\,^{\circ}C$ which is given in the literature as the crystallization temperature for one peak crystallization exotherm, [19]. As compared to the crystallization peak in [19], Figs 4 and 5 have the maximum of the transition peak shifted slightly to higher temperatures of 136 and $133\,^{\circ}C$, respectively, which are close enough to $120\,^{\circ}C$ to identify them as the crystallization transformation to the hexagonal phase. Hence, we observed in this investigation that only the thermally-treated sample DSC thermograms look similar to thermograms of a–Se obtained by vacuum processes. The very low temperature exotherm at $T_{II}^{EX} \simeq 95\,^{\circ}C$ obviously pertains to some form of early crystallization or reordering of the a–Se material as obtained by photodeposition. Since it has such a distinct sharp profile, it may be connected, for example, to a different type of crystallization such as to the α or β-form which are known to require less packing order as compared to the hexagonal phase. Also, the hexagonal phase needs a higher thermal energy to allow reordering of the softened amorphous phase to the closely packed trigonal form. How such a difference in the mechanism of the crystallization may occur at T_I^{EX} as compared to T_{II}^{EX} we may gather from the following reasons. Crystallization is a heterogeneous reaction which occurs at the phase boundaries and usually consists of two consecutive events. The first consists of atomic or molecular diffusion to the phase boundary and the second is the crystallization at the boundary [22]. Now the first crystallization peak occurring at $T_I^{EX} = 95\,^{\circ}C$ can be assigned to ring members which acquire enough energy to diffuse to the crystallization sites. It also seems to occur more favourably for the as-photodeposited material – hence ring diffusion seems to be more easily facilitated as compared to the quenched samples. We therefore speculate that since the monoclinic phase of a–Se only consists of closed rings [23], as compared to the trigonal phase which consists of parallel helical chains, the diffusion limited crystallization first causes monoclinic crystallization observed at $T_I^{EX} \simeq 95\,^{\circ}C$ and only at the higher temperatures do the helical chains become free to diffuse and allow crystallization of the hexagonal phase. Also, it is possible that the rings only need rotational structural re-adjustment to crystallize to the monoclinic form while the helical chains also need translational motion to allow hexagonal crystallization to take place. We then expect that the heating and quenching procedures change the relative populations of rings and chains in the amorphous structure. We can also determine quantitatively the relative percentage crystallinity for the samples before and after the two quenching procedures. The DSC method for determining the percentage crystallinity of a semi-crystalline material is based upon the measurement of the heat of fusion ΔH. The equation we used is

$$C \triangleq \text{Percentage crystallinity} = \frac{\Delta H}{\Delta H^*} \times 100\% \tag{1}$$

This equation relies on the reasonable assumption that ΔH is proportional to the percentage crystallinity. For trigonal Se the heat of fusion [1], ΔH^* is 1490 cal mol^{-1} hence, using the data in Table I we obtain the following results for the crystallinity of the samples whose DSC scans are given in Figs 3, 4 and 5:

$$C_1 = 73.4\%;\quad C_2 = 65.8\%;\quad C_3 = 66.5\%$$

This shows that the crystallinity or ordered degree of the virgin-photodeposited sample is considerably higher, by about 12%, as compared to the quenched or annealed samples.

4. Conclusion

The crystallization behaviour of amorphous selenium films obtained by the low temperature photodeposition process was examined. As-obtained samples produced DSC thermograms with features not previously observed for vacuum deposited a–Se films or quenched from the molten phase. We have carried out quenching and annealing processes with interesting results. The quenched specimens thermograms were quite similar to those obtained by high temperature processes. On the other hand, the specimens cooled slowly exhibited a very small glass transition peak. These features are important in understanding the

relative role of ring and chain members in the crystallization behaviour of a–Se.

Acknowledgement

The authors would like to express their appreciation to Z. Ronen and R. Barad of the CTEH for their assistance in the course of this project. Part of this work was performed at the IBM Almaden Research Center, with support and encouragement of Dr L. B. Scheiu.

References

1. W. C. COOPER and R. A. WESTBURY, in "Selenium", edited by R. A. Zingaro and W. C. Cooper (Van-Nostrand Reinhold Co., New York, 1974) pp. 87–147.
2. A. JENKINS, in "Materials Used in Semiconductor Devices", edited by C. A. Hogarth (Interscience Publications, New York, 1965) pp. 49–70.
3. C. KLASON, J. KUBAT and Ch. SOREMARK, *Koll. Zeitsch. & Zeitsch., Für Polymere* **245** (1971) 465.
4. K. VEDAM, D. L. MILLER and R. ROY, *J. Appl. Phys.* **37** (1966) 3432.
5. G. GATTOW and G. HEINRICH, *Zeitsch. für Anorg. und Allgem. chemie* **331** (1964) 284.
6. A. M. de BECDELIEVRE and J. de BECDELIEVRE, *Mater. Res. Bull.* **5** (1970) 73.
7. J. C. SCHOTTMILLER, *J. Vac. Sci. Technol.* **12** (1975) 807.
8. G. G. ROBERTS, B. S. KEATING and A. V. SHELLEY, *J. Phys. C. Solid State* **7** (1974) 1595.
9. W. C. COOPER and R. A. WESTBURY, in "Selenium", edited by R. A. Zingaro and W. C. Cooper (Van-Nostrand Reinhold Co., New York, 1974) p. 117.
10. W. C. COOPER and R. A. WESTBURY, in "Selenium", edited by R. A. Zingaro and W. C. Cooper (Van-Nostrand Reinhold Co., New York, 1974) pp. 125–142.
11. C. ORTIZ and K. A. RUBIN, *J. Mater. Res.* **3** (1988) 1196.
12. J. C. PERRON, *J. Non-Cryst. Solids* **8** (1972) 272.
13. A. PELED, D. NAOT and M. PERAKH, *J. Colloid Polym. Sci.* **266** (1988) 958.
14. P. SAALFRANK, P. OTTO and L. LADIK, *Chem. Phys. Lett.* **153** (1988) 451.
15. W. C. COOPER and R. A. WESTBURY, in "Selenium", edited by R. A. Zingaro and W. C. Cooper (Van-Nostrand Reinhold Co., New York, 1974) pp. 121–122; pp. 299–301.
16. R. KAPLOW, T. A. ROWE and B. L. AVERBACH, *Phys. Rev.* **168** (1968) 1072.
17. A. PELED, *J. Mater. Res.* **4** (1989) 177.
18. *Idem., J. Colloid Polym. Sci.* **262** (1984) 718.
19. S. O. KASAP and C. JUHASZ, *J. Mater. Sci. Lett.* **6** (1987) 397.
20. S. O. KASAP, M. WINNICKA and S. YANNACOPOULOS, *J. Mater. Res.* **3** (1989) 609.
21. P. J. FORD, G. A. SAUNDERS, E. F. LAMBSON and G. CARINI, *Phil. Mag. Lett.* **57** (1988) 201.
22. J. BURKE, in "The Kinetics of Phase Transformation in Metals" (Pergamon Press, Oxford, 1965).
23. G. G. ROBERTS, *J. Phys. C. Solid State* **7** (1974) 1597.

Received 1 November 1989
and accepted 30 May 1990